

XIX INTERNATIONAL SYMPOSIUM ON LEPTON AND PHOTON INTERACTION  
AT HIGH ENERGY  
Stanford University, August 9-14, 1999

L.G.Landsberg  
State Research Center, Institute for High Energy Physics,  
Protvino, Moscow region, Russia, 142284

**SEARCH FOR EXOTIC BARYONS WITH HIDDEN  
STRANGENESS IN THE EXPERIMENTS  
OF THE SPHINX COLLABORATION\*)  
IN DIFFRACTIVE AND COULOMB PRODUCTION  
PROCESSES**

---

\*)The SPHINX Collaboration (IHEP-ITEP):

S.V.Golovkin, A.P.Kozhevnikov, V.P.Kubarovsky, V.F.Kurshetsov, L.G.Landsberg, V.V.Molchanov, V.A.Mukhin,  
S.V.Petrenko, D.V.Vavilov, V.A.Victorov

*State Research Center, Institute for High Energy Physics, Protvino, Russia*

V.Z.Kolganov, G.S.Lomkatsi, A.F.Nilov, V.T.Smolyankin

*State Research Center, Institute of Theoretical and Experimental Physics, Moscow, Russia*

## Abstract

Experimental results of the SPHINX Collaboration on studying proton diffractive production processes are presented. Evidences for new baryon states with masses  $\gtrsim 1.8$  GeV were obtained in hyperon-kaon effective mass spectra in several reactions. New data for the diffractive reaction  $p + N \rightarrow [\Sigma^0 K^+] + N$  at  $E_p = 70$  GeV were obtained with partially upgraded SPHINX setup. The data are in a good agreement with the results of our previous study of this reaction. In the mass spectrum  $M(\Sigma^0 K^+)$  a structure at the threshold region with a mass  $\sim 1800$  MeV and a distinct  $X(2000)$  peak with  $M = 1989 \pm 6$  MeV and  $\Gamma = 91 \pm 20$  MeV are observed. Unusual features of the massive  $X(2000)$  state (narrow decay width, anomalously large branching ratio for the decay channel with strange particle emission) make it a serious candidate for cryptoexotic pentaquark baryon with hidden strangeness  $|qqqs\bar{s}\rangle$ . We also present new results on the narrow threshold structure  $X(1810)$  with  $M = 1807 \pm 7$  MeV and  $\Gamma = 62 \pm 19$  MeV which is produced in the region of very small  $p_T^2 < 0.01$  GeV<sup>2</sup>. The possibility of the Coulomb production mechanism for  $X(1810)$  is discussed.

## 1 INTRODUCTION

The last two decades have been marked by a significant increase in studies in the field of spectroscopy of hadrons, that is, the particles participating in strong interactions. It has been firmly established that hadrons are not truly elementary, but composite particles. Similar to atomic nuclei, which consist of nucleons, hadrons are bound systems composed of fundamental particles known as quarks. Quarks are those structural elements that define the variety of the hadronic matter. In addition to a fractional electric charge and baryon number, different flavors (isospin, strangeness, charm, etc.) quarks have a “strong-interaction charges” called colors.

The interactions between quarks go through the exchange of color virtual particles, gluons, in a similar way as the interactions between electric charges are effected by exchange of virtual photons. However, in contrast to neutral photons, which bear no charge and do not interact directly with each other, gluons are characterized by color “charges” and are capable of interacting not only with color quarks but between themselves, thus forming even bound gluon states — glueballs. The interaction between color quarks and gluons is described by quantum chromodynamics.

Apparently, color quarks and gluons cannot exist in a free state. Such a hypothesis is experimentally based on the long-standing unsuccessful efforts to find free quarks. Therefore, the concept of confinement (“the quark imprisonment”) arose, according to which only the particles without color charge can freely exist, the so-called “colorless” or “white” hadrons. All these hadrons are divided by their quantum numbers and their quark content into two large groups: baryons and mesons. Baryons are characterized by their baryon number  $B$  ( $B=1$  for baryons and  $B=-1$  for antibaryons) and are produced in pairs to conserve the baryon number of the whole system. Mesons have  $B=0$ . Rapid development of hadron spectroscopy has led to a significant advance in the systematics of ordinary hadrons with simplest valence quark structure:  $q\bar{q}$  for mesons and  $qqq$  for baryons.

Here, we consider only the so-called valence quarks, which determine the hadron nature and its main characteristics (quantum numbers). According to the current theoretical perceptions, well confirmed by numerous experiments, the valence quarks in a hadron are surrounded by a “cloud” of virtual quark-antiquark pairs and gluons, which are constantly emitted and absorbed by the valence quarks. This “cloud” or, as one says now, the “sea” of quark-antiquark pairs and gluons, is physical reality determining many properties of hadron (for example, space distribution of its electric charge and magnetic moment, intrinsic distribution of quark and gluon constituents over momenta, etc.).

A very important question is whether there exist “colorless” hadrons with a more complex inner valence structure, such as multiquark mesons ( $M = qq\bar{q}\bar{q}$ ) and baryons ( $B = qq\bar{q}q$ ), dibaryons ( $D = qq\bar{q}qq$ ), hybrid states ( $M = q\bar{q}g$ ), and glueballs, which are mesons composed only of gluons ( $M = gg, ggg$ ). Of course, in such new forms of hadronic matter, known as exotic hadrons, effects of the quark-gluon “sea” must also appear in addition to the valence quark and gluon structure.

The discovery of the exotic hadrons would have a far-reaching consequences for quantum chromodynamics, for the concept of confinement and for specific models of hadron structure (lattice, string, and bag models). Detailed discussions of exotic hadron physics can be found in recent reviews [1-7].

Exotic hadrons can have anomalous quantum numbers not accessible to three-quark baryons or quark-antiquark mesons (open exotic states), or even usual quantum numbers (cryptoexotic states). Cryptoexotic hadrons can be identified only by their unexpected dynamical properties (anomalously narrow decay widths, anomalous decay branching ratios and so on).

As is clear from review papers [1-7], in the last decade searches for exotic mesons have led to a considerable advance in this field. Several new states have been observed whose properties cannot be explained in the framework of naive quark model of ordinary mesons with  $q\bar{q}$  valence quark structure. These states are serious candidates for exotic mesons (most of them are of cryptoexotic type).

At the same time the situation for exotic baryons is far from being clear. There are also some examples of possible unusual baryon resonances [8-11], but these data are not sufficiently precise and are not supported by some new experimental results [2,12-16].

Extensive studies of the diffractive baryon production and search for cryptoexotic pentaquark baryons with hidden strangeness ( $B_\phi = |qqqs\bar{s}\rangle$ , here  $q = u, d$  quarks) are being carried out by the SPHINX Collaboration at the IHEP accelerator with 70 GeV proton beam. This program was described in detail in reviews [2].

The recent data of the SPHINX experiment [16-25] gave new important evidence of possible existence of cryptoexotic baryons with hidden strangeness  $X(2050)^+ \rightarrow \Sigma(1385)^0 K^+$  and  $X(2000)^+ \rightarrow \Sigma^0 K^+$ . We shall summarize these data in Section 3, after a general description of the nature and expected properties of cryptoexotic baryons, as well as some promising ways for their production and observation. There were also the SPHINX results in favor of strong violation of the OZI rule in proton diffractive dissociation reactions [26-28] which may be connected with direct strangeness in the nucleon quark structure.

## 2 EXOTIC BARYONS AND POSSIBLE MECHANISMS OF THEIR PRODUCTION

There arise three main questions tightly connected with the exotic searches in the SPHINX experiments:

1. How to identify cryptoexotic  $B_\phi = |qqqs\bar{s}\rangle$  baryons without open exotic values of their quantum numbers and how to distinguish them from several dozens of well-known  $N^*$  and  $\Delta$  isobars?
2. How to produce the exotic baryons in the most effective way?
3. How to reduce background processes and to make easier the exotic baryon observation?

We will try to find some qualitative answers to these questions because of the lack of theoretical models for the description of exotic hadrons.

## 2.1 Properties of Exotic Baryons with Hidden Strangeness

As has been stated before, cryptoexotic baryons do not have external exotic quantum numbers, and their complicated internal valence structure can be established only indirectly by examining their unusual dynamical properties that are quite different from those of ordinary baryons  $|qqq\rangle$ . In this connection, we consider the properties of multiquark baryons with hidden strangeness  $|qqqs\bar{s}\rangle$ .

If such cryptoexotic baryon structure consists of two color parts spatially separated by a centrifugal barrier, its decays into the color-singlet final states may be suppressed because of a complicated quark rearrangement in decay processes. The properties of multiquark exotic baryons with the internal color structure

$$|qqqq\bar{q}\rangle_{1c} = |(qqq)_{8c} \times (q\bar{q})_{8c}\rangle \quad (1)$$

(color octet bonds) or

$$|qqqq\bar{q}\rangle_{1c} = |(qq\bar{q})_{\overline{6c}} \times (qq)_{6c}\rangle \quad (2)$$

(color sextet-antisextet bonds) are discussed in [29-32]. Here, subscripts 1c, 8c, and so on specify representations of the color  $SU(3)_c$  group. If the mass of a nonstrange baryon with hidden strangeness is above the threshold for decay modes involving strange particles in final states, the main decay channels must be of the type

$$B_\phi = |qqqs\bar{s}\rangle \rightarrow YK + k\pi \quad (3)$$

( $k=0, 1, \dots$ ). Another possibility is associated with the decays

$$B_\phi = |qqqs\bar{s}\rangle \rightarrow \phi N(\eta N; \eta' N) + k\pi. \quad (4)$$

which involve the emission of particles with a significant  $s\bar{s}$  component in their valence-quark structure. It should also be emphasized that  $\eta$  and, particularly,  $\eta'$  mesons are strongly coupled to gluon fields and, hence, to the states with an enriched gluon component. Therefore, baryon decays of the type  $B \rightarrow N\eta$ ,  $N\eta'$  may be specific decay modes for hybrid baryons (see, for example, [2]).

The nonstrange decays of baryons with hidden strangeness,  $B_\phi \rightarrow N + k\pi$ , must be suppressed by the OZI rule. Thus, the effective phase-space factors for the decays of the massive baryons  $B_\phi$  would be significantly reduced because of this OZI suppression (owing to a high mass threshold for the allowed decays  $B_\phi \rightarrow YK$  with respect to the suppressed decay  $B_\phi \rightarrow N\pi$ ,  $\Delta\pi$ ). The mechanism of quark rearrangement of color clusters in the decays of particles with complicated inner structure of type (1) or (2) can further reduce the decay width of cryptoexotic baryons and make them anomalously narrow (their widths may become as small as several tens of MeV). Here, theoretical predictions are rather uncertain. For this reason, only experiments can answer conclusively the question of whether such narrow baryon resonances with hidden strangeness really exist.

Thus, it is desirable to perform systematic searches for the cryptoexotic baryons  $B_\phi$  with anomalous dynamical features listed below.

(i) The dominant OZI-allowed decay modes of the baryons  $B_\phi$  are those with strange particles in the final states:

$$R(|qqqs\bar{s}\rangle = BR[|qqqs\bar{s}\rangle \rightarrow YK] / BR[|qqqs\bar{s}\rangle \rightarrow p\pi\pi; \Delta\pi] \gtrsim 1. \quad (5)$$

For ordinary  $|qqq\rangle$  isobars  $R(\Delta; N^*) \sim (\text{several } \%)$  [33].

ii) The cryptoexotic baryons  $B_\phi$  can simultaneously possess a large mass ( $M > 1.8 - 2.0$  GeV) and a narrow decay width ( $\Gamma \leq 50 - 100$  MeV). This is due to a complicated internal color

structure of these baryons, which leads to a significant quark rearrangement of color clusters in decay processes, and due to a limited phase space for the OZI-allowed decays  $B_\phi \rightarrow YK$ . At the same time, typical decay widths of the well-established  $|qqq\rangle$  isobars with similar masses are not less than 300 MeV.

## 2.2 Diffractive Production Mechanism and Search for Exotics

It was emphasized in a number of studies [1,2,8,10,30,32,34] that diffractive production processes featuring Pomeron exchange offer new possibilities in searches for exotic hadrons. Originally, interest was focused on the model of Pomeron with a small cryptoexotic ( $qq\bar{q}\bar{q}$ ) component [30,32]. According to modern concepts, the Pomeron is a multigluon system owing to which exotic hadrons can be produced in gluon-rich diffractive processes (see Fig. 1).

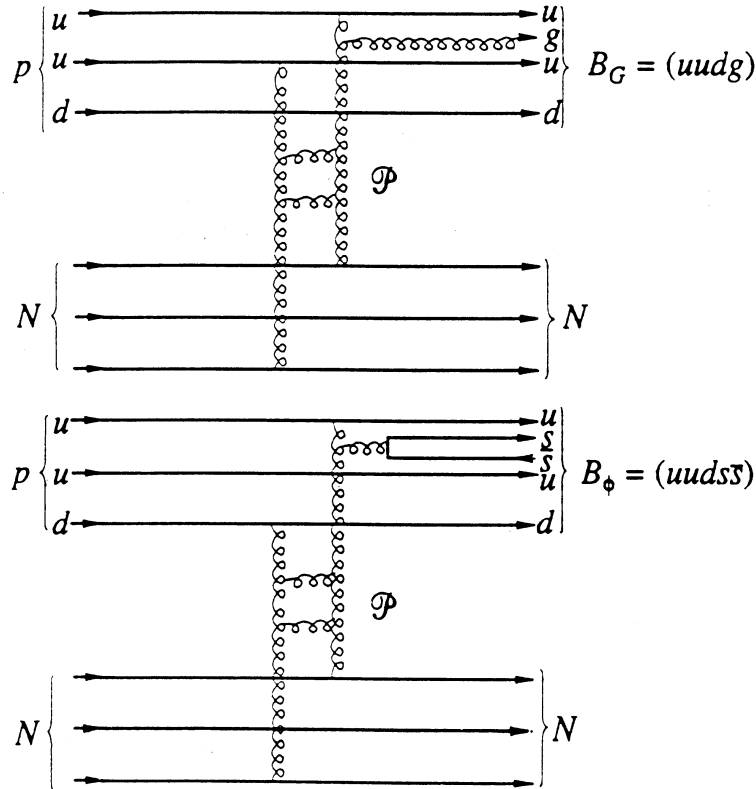


Figure 1: Diagrams for exotic baryon production in the diffraction processes with the Pomeron exchange. The Pomeron  $\mathcal{P}$  is a multigluon system.

It is apparent that only the states with the same charge and flavor as those of the primary hadrons can be produced in diffractive processes. Moreover, there are some additional restrictions on the spin and parity of the formed hadrons which are stipulated by the Gribov-Morrison selection rule. According to this rule, the change in parity  $\Delta P$  occurring as a result of the transition from the primary hadron to the diffractively produced hadronic system, is connected with the corresponding change in the spin  $\Delta J$  through the relation  $\Delta P = (-1)^{\Delta J}$ . For example, because of this rule, in the proton diffractive dissociation (for proton  $J^P = 1/2^+$ ), only baryonic states with natural sets of quantum numbers  $1/2^+, 3/2^-, 5/2^+, 7/2^-,$  etc. can be excited. The Gribov-Morrison selection rule is not a rigorous law and has an approximate character.

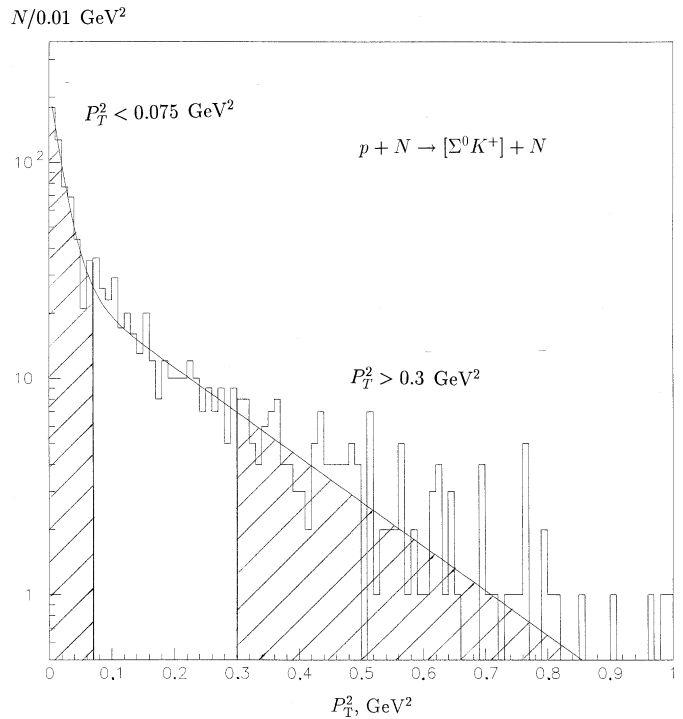
The Pomeron exchange mechanism in diffractive production reactions can induce the coherent processes on the target nucleus. In such processes the nucleus acts as discrete unit. Coherent processes can be easily identified by the transverse momentum spectrum of the final state particle system. They manifest themselves as diffractive peaks with large values of the slope parameters determined by the size of the nucleus:  $dN/dP_T^2 \simeq \exp(-bP_T^2)$ , where  $b \simeq 10 A^{2/3} \text{ GeV}^{-2}$ . Owing to the difference in the absorption of single-particle and multiparticle objects in nuclei, coherent processes could serve as an effective tool for separation of resonance production against non-resonant multiparticle background (see, e.g. [35]).

The conditions for coherent reactions are destroyed by absorption processes in nuclei. Thus, the coherent suppression of nonresonant background takes place:

$$\frac{\sigma_{coh}(res)}{\sigma_{coh}(nonres. BG)} > \frac{\sigma_{noncoh}(res)}{\sigma_{noncoh}(nonres. BG)}. \quad (6)$$

The separation of coherent reactions can be achieved by studying  $dN/dP_T^2$  distributions for processes under investigation.

Figure 2:  $dN/dP_T^2$  distribution for typical diffractive production reaction ( $p + N \rightarrow [\Sigma^0 K^+] + N$ ). The  $P_T^2$ -regions for coherent reaction on carbon nuclei ( $P_T^2 < 0.075 \div 0.1 \text{ GeV}^2$ ) and for non-peripheral processes ( $P_T^2 > 0.3 \text{ GeV}^2$ ) are shown.



As is seen from  $dN/dP_T^2$  spectra in the SPHINX experiments, there are strong narrow forward cones in these distributions with the slope  $b \gtrsim 50 \text{ GeV}^{-2}$ , which correspond to a coherent diffractive production on carbon nuclei (see, for example, Fig. 2). For identification of the coherently produced events we used “soft” transverse momentum cut  $P_T^2 < 0.075 \div 0.1 \text{ GeV}^2$ . With this cut noncoherent background in the event sample can be as large as 30÷40%. It is possible to reduce this background with more stringent  $P_T^2$  cut at the cost of some decrease of the signal statistics.

### 2.3 Processes with Large Transverse Momenta

As was discussed above, coherent diffractive production reactions with small transverse momenta seem quite promising for the search for exotic hadrons, but, of course, they do not exhaust the exist-

ing opportunities. Certainly, these searches can be also performed for all diffractive-type processes (e.g. without coherent cuts for small  $P_T^2$ ). And of special interest is the study of nonperipheral production reactions which can be the most effective way to seek for certain exotic states, especially those that are formed at short ranges and are characterized by broad enough transverse momentum distributions. In this case, the most favorable conditions for identifying exotic hadrons are achieved at higher transverse momenta ( $P_T^2 > 0.3 - 0.5 \text{ GeV}^2$ ), where the background from peripheral processes is strongly suppressed. For instance, the unusually narrow meson states  $X(1740) \rightarrow \eta\eta$  [36] and  $X(1910) \rightarrow \eta\eta'$  [37] were observed in studying the charge-exchange reactions  $\pi^- + p \rightarrow [\eta\eta] + \Delta^0$  and  $\pi^- + p \rightarrow [\eta\eta'] + n$  after the selection of events with  $P_T^2 \geq 0.3 \text{ GeV}^2$ . These anomalous states are good candidates for cryptoexotic mesons. The rescattering mechanism involving multipomeron exchange in the final state (a gluon-rich process) may explain  $X(1740)$  and  $X(1910)$  nonperipheral production [38].

In the very high primary energy region which, for example, corresponds to the search for exotic states with heavy quarks, diffractive production reactions with rescattering can be used, instead of the charge-exchange processes with rescattering (see the diagram in Fig. 3). The cross sections of these diffractive processes also do not die out with energy rise. The nonperipheral  $P_T^2$  region for these processes is shown in Fig. 2.

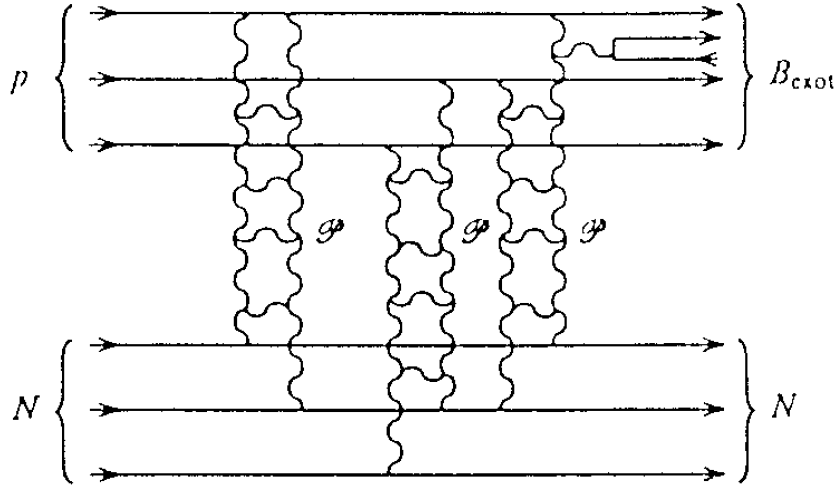


Figure 3: Diagram for diffractive – type reaction with multiple Pomeron rescattering (these processes might be significant at  $P_T^2 \gtrsim 0.3 \text{ GeV}^2$ ).

## 2.4 Electromagnetic Mechanism

The search for exotic hadrons with hidden strangeness can be also carried out in another type of hadron production processes caused by electromagnetic interactions. The example of such process is the formation reaction with s-channel resonance photoproduction of strange particles

$$\gamma + N \rightarrow |qqq\bar{s}\bar{s}\rangle \rightarrow YK \quad (7)$$

(see diagram in Fig. 4a). It is possible in principle to study the s-channel resonance production by detailed energetic scanning of the cross sections and angular distributions for (7) and by performing the subsequent partial-wave analysis. As is seen from Fig. 4a and from VDM (with its significant coupling of photon with  $s\bar{s}$  pair through  $\phi$ -meson), reaction (7) can provide a natural way to embed

the  $s\bar{s}$  quark pair into intermediate resonance state and to produce the exotic baryon with hidden strangeness.

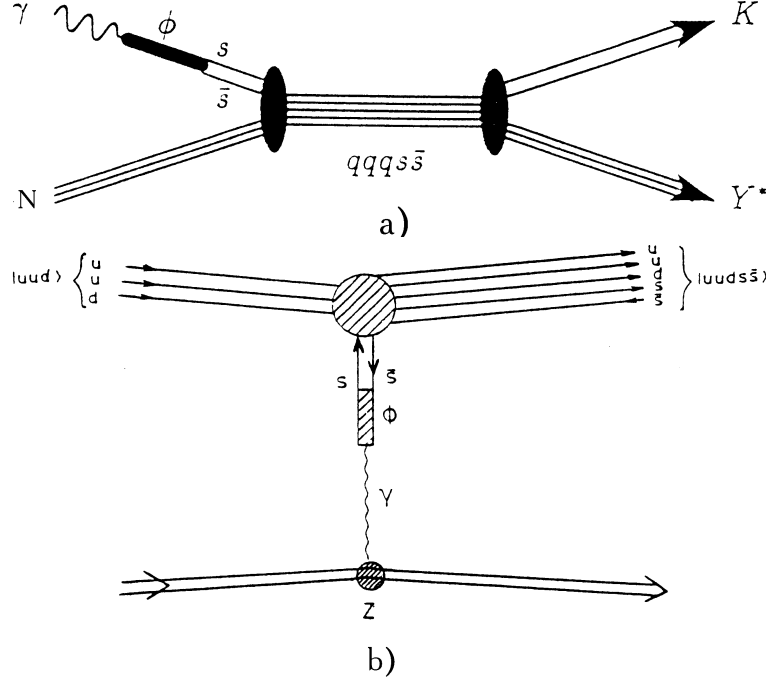


Figure 4: Electromagnetic mechanisms for production of exotic baryons with hidden strangeness: a) formation reaction with  $s$ -channel resonance photoproduction; b) Coulomb production reaction  $h + (Z, A) \rightarrow a + (Z, A)$ .

The existing data on reactions (7) are rather poor and insufficient for such systematical studies. But one can hope that good data would be produced in the near future in the experiments on strong current electron accelerators CEBAF and ELSA (see, for example, [39]).

Electromagnetic production of exotic hadrons can be searched for not only in the resonance photoproduction reactions but in the collisions of the primary hadrons with virtual photons of the Coulomb field of the target nuclei [40-44], e.g. in the Primakoff production reactions

$$h + Z \rightarrow a + Z \quad (8)$$

(see diagram in Fig. 4b). The Coulomb production mechanism plays the leading role in the region of very small transfer momenta, where it dominates over the strong interaction process [40-42]. The total cross section of the Coulomb reaction (8) is

$$\sigma[h + Z \rightarrow a + Z]|_{Coulomb} \simeq \sigma_o \frac{2J_a + 1}{2J_h + 1} \Gamma(a \rightarrow h + \gamma). \quad (9)$$

The value  $\sigma_o$  is obtained in the QED calculations. In the narrow width approximation for the resonance  $a$   $\sigma_o$  has the form

$$\sigma_o = 8\pi\alpha Z^2 \left[ \frac{M_a}{M_a^2 - m_h^2} \right]^3 \int_{q_{min}^2}^{q^2} \frac{[q^2 - q_{min}^2]}{q^4} |F_z(q^2)|^2 dq^2 \quad (10)$$



Here  $Z$  is the charge of nucleus;  $\alpha = 1/137$  is the narrow structure constant;  $\Gamma(a \rightarrow h + \gamma)$  is the radiative width of  $a$ ;  $J_a$ ,  $J_h$  and  $M_a$ ,  $m_h$  are the spins and masses of  $a$  and  $h$  particles;  $F_z(q^2)$  is the electromagnetic formfactor of nucleus;  $q_{min}^2 = [(M_a^2 - m_h^2)/2E_h]^2$  is the minimum square momentum transfer  $q^2$ ;  $E_h$  is the primary hadron energy. In the high energy region  $q_{min}^2$  is very small and  $q^2 = P_T^2 + q_{min}^2 \simeq P_T^2$ .

It must be borne in mind that in the Coulomb production reactions with primary protons one studies the same processes as in ordinary photoproduction reactions. But the Coulomb production in the experiments with unstable primary particles (pions, kaons, hyperons) opens the unique possibility to study the photoproduction reactions with these unstable “targets”.

### 3 THE EXPERIMENTS WITH THE SPHINX SETUP

The search for exotic baryons with hidden strangeness was performed in the experiments on the proton beam of the 70 GeV IHEP accelerator with the SPHINX spectrometer. The SPHINX setup includes the following basic components:

1. A wide aperture magnetic spectrometer with proportional wire chambers, drift chambers, drift tubes, scintillator hodoscopes.
2. Multichannel  $\gamma$ -spectrometer with lead-glass Cherenkov total absorption counters.
3. A system of gas Cherenkov detectors for identification of secondary charged particles (including a RICH detector with photomatrix equipped with 736 small phototubes; this is the first counter of this type used in the experiments).
4. Trigger electronics, data acquisition system and on-line control system.

The SPHINX spectrometer works in the proton beam with energy  $E_p=70$  GeV and intensity  $I \approx (2 \div 3) \cdot 10^6$  p/cycle. The measurements were performed with a polyethylene target to optimize the acceptance, sensitivity and secondary photon losses.

The first version of the SPHINX setup was described in [12]. The next version of this setup after partial modification (with a new  $\gamma$ -spectrometer and with better conditions for  $\Lambda$  and  $\Sigma^0$  identification) was discussed in [21].

To separate different exclusive reactions, a complete kinematical reconstruction of events was performed by taking into account information from the tracking detectors, from the magnetic spectrometer, from the  $\gamma$ -spectrometer, and from all Cherenkov counters of the SPHINX setup. At the final stage of this reconstruction procedure, the reactions under study were identified by examining the effective-mass spectra for subsystems of secondary particles.

Several photon-induced diffractive production processes were studied in the experiments of the SPHINX Collaboration [12-25;27;28]:

$$p + N \rightarrow [pK^+K^-] + N, \quad (11)$$

$$\rightarrow [p\phi] + N \quad (12)$$

$$\quad \hookrightarrow K^+K^-$$

$$\rightarrow [\Lambda(1520)K^+] + N, \quad (13)$$

$$\quad \hookrightarrow K^-p$$

$$\rightarrow [\Sigma^*(1385)^0K^+] + N, \quad (14)$$

$$\quad \hookrightarrow \Lambda\pi^0$$

$$\rightarrow [\Sigma^*(1385)^0K^+] + N + (neutrals), \quad (15)$$

$$\begin{aligned} & \hookrightarrow \Lambda \pi^o \\ \rightarrow & [\Sigma^o K^+] + N, \end{aligned} \quad (16)$$

$$\begin{aligned} & \hookrightarrow \Lambda \gamma \\ \rightarrow & [\Sigma^+ K^o] + N \\ & \hookrightarrow p \pi^0 \hookrightarrow \pi^+ \pi^- \end{aligned} \quad (17)$$

$$\begin{aligned} \rightarrow & [p \eta] + N, \\ & \hookrightarrow \pi^+ \pi^- \pi^o \end{aligned} \quad (18)$$

$$\begin{aligned} \rightarrow & [p \eta'] + N, \\ & \hookrightarrow \pi^+ \pi^- \eta \rightarrow \pi^+ \pi^- 2\gamma \end{aligned} \quad (19)$$

$$\begin{aligned} \rightarrow & [p \omega] + N, \\ & \hookrightarrow \pi^+ \pi^- \pi^o \end{aligned} \quad (20)$$

$$\rightarrow [p \pi^+ \pi^-] + N, \quad (21)$$

$$\begin{aligned} \rightarrow & [\Delta^{++} \pi^-] + N, \\ & \hookrightarrow p \pi^+ \end{aligned} \quad (22)$$

and several other processes. Here N is nucleon or C nucleus for the coherent processes. The separation of coherent diffractive processes is obtained by studying their  $dN/dP_T^2$  distributions, as is shown in Fig. 2.

#### 4 PREVIOUS DATA ON THE COHERENT DIFFRACTIVE REACTIONS $p + C \rightarrow [\Sigma^o K^+] + C$ AND $p + C \rightarrow [\Sigma^*(1385)^o K^+] + C$

One of the major results obtained with the SPHINX setup was the study of  $\Sigma^o K^+$  system produced in diffractive process (16).

These data were obtained in two different runs on the SPHINX facility:

- a) the first run with the old version of this setup (“old run”, [12,17-20]);
- b) the second run with partially upgraded SPHINX apparatus (“new run” [21-23]). As a result of this upgrading the detection efficiency and purity of  $\Lambda$  and  $\Sigma^o$  events were significantly increased.

The main results of these measurements can be summarized as follows:

1. Old [16-20] and new [21-23] data from coherent diffractive reaction (16) were obtained under different experimental conditions, with a significantly modified apparatus, with different background and systematics. Nevertheless, the  $\Sigma^o K^+$  invariant mass spectra from both runs are in a good agreement which makes them more reliable.

2. The combined mass spectrum  $M(\Sigma^o K^+)$  for coherent reaction (16) from the old and new data (with  $P_T^2 < 0.1 \text{ GeV}^2$ ) is presented in Fig.5. This spectrum is dominated by the X(2000) peak with parameters in Table 1.

3. There is also some near threshold structure in this  $M(\Sigma^o K^+)$  spectrum in the region of  $\sim 1800 \text{ MeV}$  (see Fig.5 and Table 1). Such a shape of the  $\Sigma^o K^+$  mass spectrum (with an additional structure near the threshold) proves that the X(2000) peak cannot be explained by a non-resonant Deck-type diffractive singularity. Therefore, most likely this peak has a resonant nature.

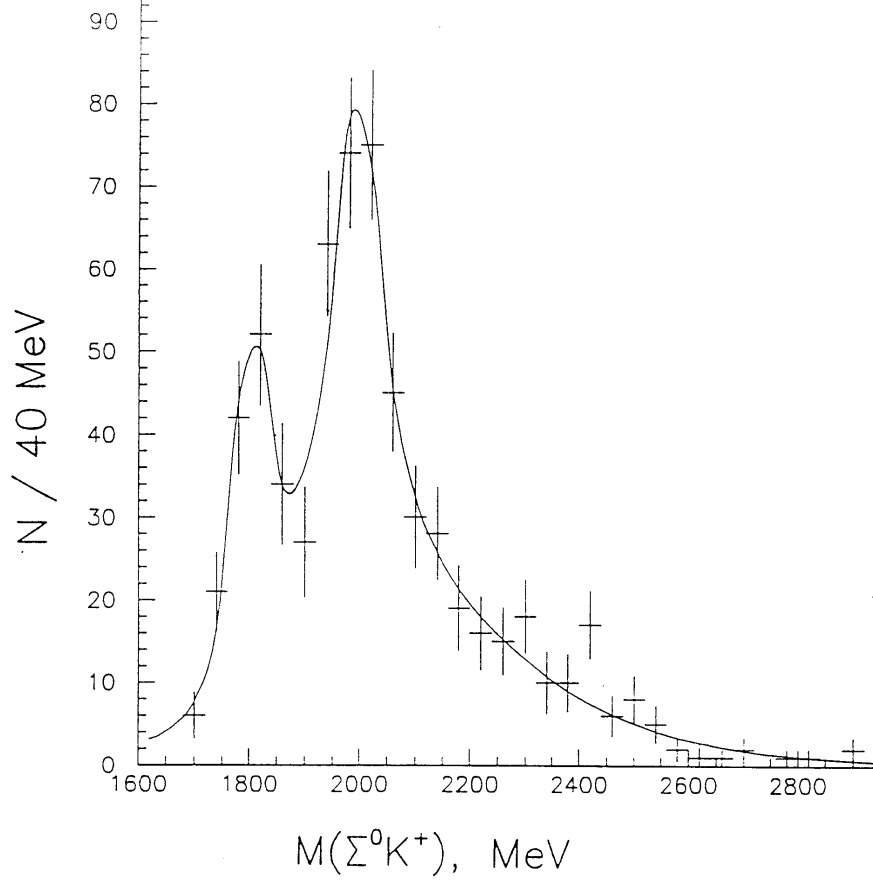


Figure 5: Combined mass spectrum  $M(\Sigma^0 K^+)$  for coherent diffractive reaction (16) in old and new runs on the SPHINX setup ( $P_T^2 < 0.1 \text{ GeV}^2$ ). The parameters of  $X(2000)$  peak in this spectrum are:  $M = 1997 \pm 7 \text{ MeV}$ ;  $\Gamma = 91 \pm 17 \text{ MeV}$ .

Table 1: The main results of the previous SPHINX data for coherent diffractive reactions  $p+C \rightarrow [\Sigma^0 K^+] + C$  and  $p + C \rightarrow [\Sigma^*(1385)^0 K^+] + C$

- 
1. Coherent diffractive production reaction  $p + C \rightarrow [\Sigma^0 K^+] + C$  with coherent cut  $P_T^2 < 0.1 \text{ GeV}^2$  was studied in the old and new runs. The combined mass spectrum  $M(\Sigma^0 K^+)$  is presented on Fig. 5. This spectrum is dominated by X(2000) state with parameters

$$\left. \begin{aligned} M &= 1997 \pm 7 \text{ MeV}, \\ \Gamma &= 91 \pm 17 \text{ MeV}, \\ \text{statistical significance of the peak is } &7 \text{ s.d.} \end{aligned} \right\}.$$

- 
2. There are also some near threshold structure X(1810), which is produced only in the region of very small  $P_T^2 (\lesssim 0.01 \div 0.02 \text{ GeV}^2)$ . The parameters of this peak are

$$M = 1812 \pm 7 \text{ MeV},$$

$$\Gamma = 56 \pm 16 \text{ MeV}.$$

- 
3. Coherent diffractive production reaction  $p + C \rightarrow [\Sigma^*(1385)K^+] + C$  with tight coherent cut  $P_T^2 < 0.02 \text{ GeV}^2$  was studied in the old run ([12;17-20]). The mass spectra of  $M[\Sigma^*(1385)^0 K^+]$  are in Fig. 6. The peak was observed in these spectra with average value of parameters

$$\left. \begin{aligned} M &= 2052 \pm 6 \text{ MeV} \\ \Gamma &= 35_{-35}^{+22} \text{ MeV} \\ \text{(with the account of the apparatus mass resolution);} \\ \text{statistical C.L. of the peak } &\geq 5 \text{ s. d.} \end{aligned} \right\}.$$

- 
4. The data of (14) and (16) were analyzed together with the data from (21) and (22) to obtain the branching ratios of different decay channels (with strange particles and without strange particle in final state). The lower limits of the ratios were obtained from this comparative analysis (with 95% C.L.):

$$R_1 = \frac{BR\{X(2050)^+ \rightarrow [\Sigma^*(1385)K]^+\}}{BR\{X(2050)^+ \rightarrow [\Delta(1232)\pi]^+\}} > 1.7$$

$$R_2 = \frac{BR\{X(2050)^+ \rightarrow [\Sigma^*(1385)K]^+\}}{BR\{X(2050)^+ \rightarrow p\pi^+\pi^-\}} > 2.6$$

$$R'_2 = \frac{BR\{X(2050)^+ \rightarrow \Sigma^*(1385)^0 K^+\}}{BR\{X(2050)^+ \rightarrow p\pi^+\pi^-\}} > 0.86$$

$$R_3 = \frac{BR\{X(2000)^+ \rightarrow [\Sigma K]^+\}}{BR\{X(2000)^+ \rightarrow [\Delta(1232)\pi]^+\}} > 0.83$$

$$R_4 = \frac{BR\{X(2000)^+ \rightarrow [\Sigma K]^+\}}{BR\{X(2000)^+ \rightarrow p\pi^+\pi^-\}} > 7.8$$

$$R'_4 = \frac{BR\{X(2000)^+ \rightarrow \Sigma^0 K^+\}}{BR\{X(2000)^+ \rightarrow p\pi^+\pi^-\}} > 2.6.$$


---

A strong influence of  $P_T^2$  cut for the production of this X(1810) state was established: this structure is produced only at very small  $P_T^2 (\lesssim 0.01 \div 0.02 \text{ GeV}^2)$  — see below.

We have also some data in studying the  $\Sigma^*(1385)^0 K^+$  system in reaction (14), which were obtained only in the old run (data on this reaction from the new run are now in process of analysis). Coherent events of (14) were singled out in the analysis of  $dN/dP_T^2$  distribution as a strong forward peak with the slope  $b \gtrsim 50 \text{ GeV}^{-2}$ . In order to reduce the noncoherent background and to obtain the  $\Sigma(1385)^0 K^+$  mass spectrum for the “pure” coherent production reaction on carbon nuclei a “tight” requirement  $P_T^2 < 0.02 \text{ GeV}^2$  was imposed and the mass spectra of  $\Sigma(1385)^0 K^+$  for the coherent events of (14) were obtained (see, for example, Fig. 6). In these spectra some very narrow

structure  $X(2050)$  was observed. The fits of the spectra with Breit-Wigner peaks and polynomial smooth background were carried out, and the average values for the main parameters of  $X(2050)$  structure are presented in Table 1. Certainly, one needs further confirmation of the existence of  $X(2050)$  in the new data with increased statistics. Up to now it is impossible also to exclude completely the feasibility for  $X(2000)$  and  $X(2050)$  to be in fact two different decay modes of the same state.

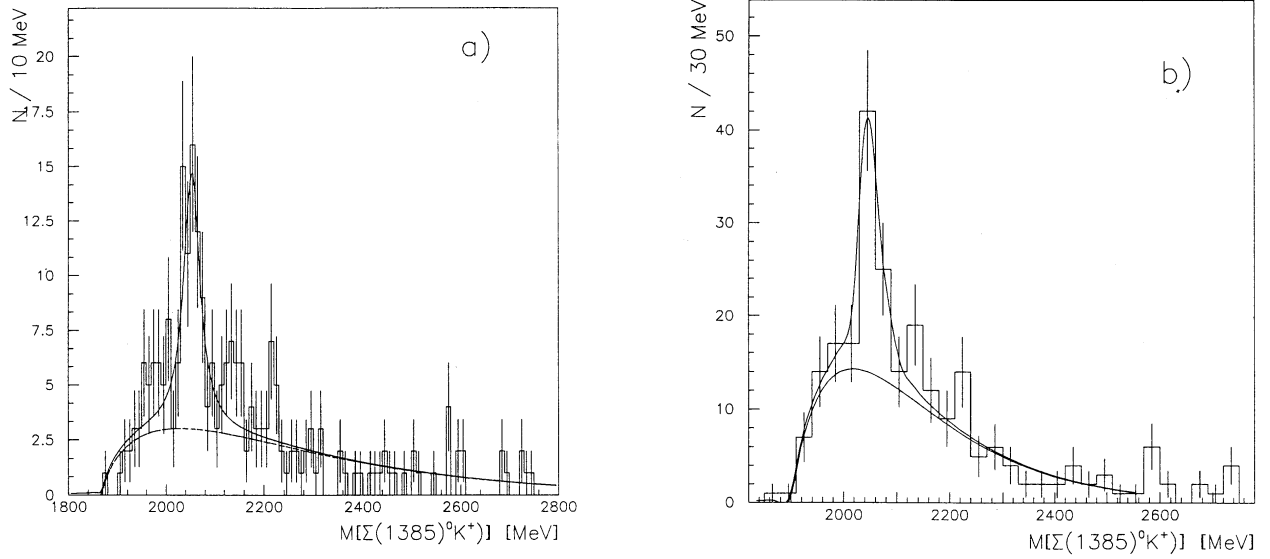


Figure 6: Invariant mass spectra  $M[\Sigma^*(1385)^0 K^+]$  in the coherent reaction (14) at tight transverse-momentum cut  $P_T^2 < 0.02$  GeV<sup>2</sup> for various bin widths: a)  $\Delta M = 10$  MeV; b)  $\Delta M = 30$  MeV. The spectra are fitted to the sum of a smooth polynomial background and  $X(2050)$  Breit-Wigner peak. The parameters of  $X(2050)$  peak are: a)  $M = 2053 \pm 4$  MeV,  $\Gamma = 40 \pm 15$  MeV; b)  $M = 2053 \pm 5$  MeV,  $\Gamma = 35 \pm 16$  MeV.

In studying coherent reactions (21)  $p + C \rightarrow [p\pi^+\pi^-] + C$  and (22)  $p + C \rightarrow [\Delta(1232)^{++}\pi^-] + C$  under the same kinematical conditions as of processes (14) and (16) a search for other decays channels of the  $X(2000)$  and  $X(2050)$  baryons was performed [18,19]. No peaks in 2 GeV mass range were observed in the mass spectra of  $p\pi^+\pi^-$  and  $\Delta(1232)^{++}\pi^-$  systems produced in reactions (21) and (22), respectively. Lower limits on the corresponding decay branching ratios  $R$  (see (5)) were obtained from this comparative analysis:

$$R[X(2000); X(2050)] \gtrsim 1 \div 10 \quad (95\% \text{ C.L.}) \quad (23)$$

(more details are in Table 1).

The isotopic relations between the decay amplitudes of  $I = 1/2$  particles were assumed in these calculations (the  $X(2000)$  and  $X(2050)$  states belong to isodoublets since they are produced in a diffractive dissociation of proton). In accordance with these relations

$$BR[X_{I=1/2}^+ \rightarrow \Sigma^0 K^+] = \frac{1}{3} BR[X_{I=1/2}^+ \rightarrow (\Sigma K)^+] \quad (24)$$

$$BR[X_{I=1/2}^+ \rightarrow \Delta^{++}\pi^-] = \frac{1}{2} BR[X_{I=1/2}^+ \rightarrow (\Delta\pi)^+] \quad (25)$$

The ratios  $R_1 - R_4$  of the widths of the  $X(2000)$  and  $X(2050)$  decays into strange and nonstrange particles are much larger than those for ordinary ( $qqq$ )-isobars [18,33].

A narrow width of the  $X(2000)$  and  $X(2050)$  baryon states as well as anomalously large branching ratios for their decay channels with strange particle emission (large values of  $R$ ) are the reasons to consider these states as serious candidates for cryptoexotic baryons with a hidden strangeness  $|uuds\bar{s}\rangle$ .

## 5 NEW ANALYSIS OF THE DATA FOR REACTION $p + N \rightarrow [\Sigma^0 K^+] + N$

In what follows we present the results of a new analysis of the data obtained in the run with partially upgraded SPHINX spectrometer where conditions for  $\Lambda$  and  $\Sigma^0$  separation were greatly improved as compared with an old version of this setup. The key element of the new analysis lays in a detailed study of the  $\Sigma^0 \rightarrow \Lambda + \gamma$  decay separation, which makes it possible to reach the reliable identification of this decay and reaction (16) with the increased efficiency in comparison with the previous analysis of [21].

In this new analysis the data for (16) were studied with different criteria for  $\Sigma^0 \rightarrow \Lambda + \gamma$  separation (with larger efficiency and larger background or with the reduced background at the price of lower efficiency). We will designate these different criteria for photon separation as soft, intermediate and strong photon cuts (the details will be presented in [45]). Reaction (16) was studied in different kinematical regions. It was found that improved background conditions were important for the investigation of the region of small mass  $M(\Sigma^0 K^+)$  and very small transverse momenta.

The effective mass spectra  $M(\Sigma^0 K^+)$  in  $p + N \rightarrow [\Sigma^0 K^+] + N$  for all  $P_T^2$  are presented in Fig. 7. The peak of  $X(2000)$  baryon state with  $M = 1986 \pm 6$  MeV and  $\Gamma = 98 \pm 20$  MeV is seen very clearly in these spectra with a very good statistical significance. Thus, the reaction

$$p + N \rightarrow \begin{array}{l} X(2000) + N, \\ \quad \quad \quad \hookrightarrow \Sigma^0 K^+ \end{array} \quad (26)$$

is well separated in the SPHINX data. The cross section for  $X(2000)$  production in (26) is:

$$\sigma[p + N \rightarrow X(2000) + N] \cdot BR[X(2000) \rightarrow \Sigma^0 K^+] = 95 \pm 20 \text{ nb/nucleon} \quad (27)$$

(with respect to one nucleon under the assumption of  $\sigma \propto A^{2/3}$ , e.g. for the effective number of nucleons in carbon nucleus equal to 5.24). The parameters of  $X(2000)$  are not sensitive to the different photon cuts, as is seen from Table 2. The  $dN/dP_T^2$  distribution for reaction (26) is shown in Fig. 8. From this distribution the coherent diffractive production reaction on carbon nuclei is identified as a diffraction peak with the slope  $b \simeq 63 \pm 10 \text{ GeV}^{-2}$ . The cross section for coherent reaction is determined as

$$\begin{aligned} \sigma[p + C \rightarrow X(2000)^+ + C]_{\text{Coherent}} \cdot BR[X(2000)^+ \rightarrow \Sigma^0 K^+] = \\ = 260 \pm 60 \text{ nb/C nucleus.} \end{aligned} \quad (28)$$

Table 2: Data on  $M(\Sigma^0 K^+)$  in reaction  $p + N \rightarrow [\Sigma^0 K^+] + N$ ,  $\Sigma^0 \rightarrow \Lambda \gamma$  with different photon cuts (for all  $P_T^2$ )

Photon cut		Soft	Intermediate	Strong
$N$ events in $X(2000)$ peak		$430 \pm 89$	$301 \pm 71$	$190 \pm 47$
Correction factor for photon efficiency		1.0	1.4	2.25
Parameters of $X(2000)$				
$M$ (MeV)	weighted spectrum	$1986 \pm 6$	$1991 \pm 8$	$1988 \pm 6$
	measured spectrum	$1988 \pm 5$	$1994 \pm 7$	$1990 \pm 6$
$\Gamma$ (MeV)	weighted spectrum	$98 \pm 20$	$96 \pm 26$	$68 \pm 21$
	measured spectrum	$84 \pm 20$	$94 \pm 21$	$68 \pm 20$
$\sigma[p + N \rightarrow X(2000) + N] \cdot$ $\cdot BR[X(2000) \rightarrow \Sigma^0 K^+]$ (nb/nucleon)		$100 \pm 19$	$93 \pm 25$	$91 \pm 21$
Average values	$\langle M \rangle$ MeV	$1989 \pm 6$		
	$\langle \Gamma \rangle$ MeV	$91 \pm 20$		
	$\langle \sigma[p + N \rightarrow X(2000) + N] \cdot$ $\cdot BR[X(2000) \rightarrow \Sigma^0 K^+]$ nb/nucleon	$95 \pm 20$ (statist.) $\pm 20$ (system.)		
	$\langle \sigma[p + C \rightarrow X(2000) + C] \cdot$ $\cdot BR[X(2000) \rightarrow \Sigma^0 K^+]$ nb/C nucleus	$285 \pm 60$ (statist.) $\pm 60$ (system.)		

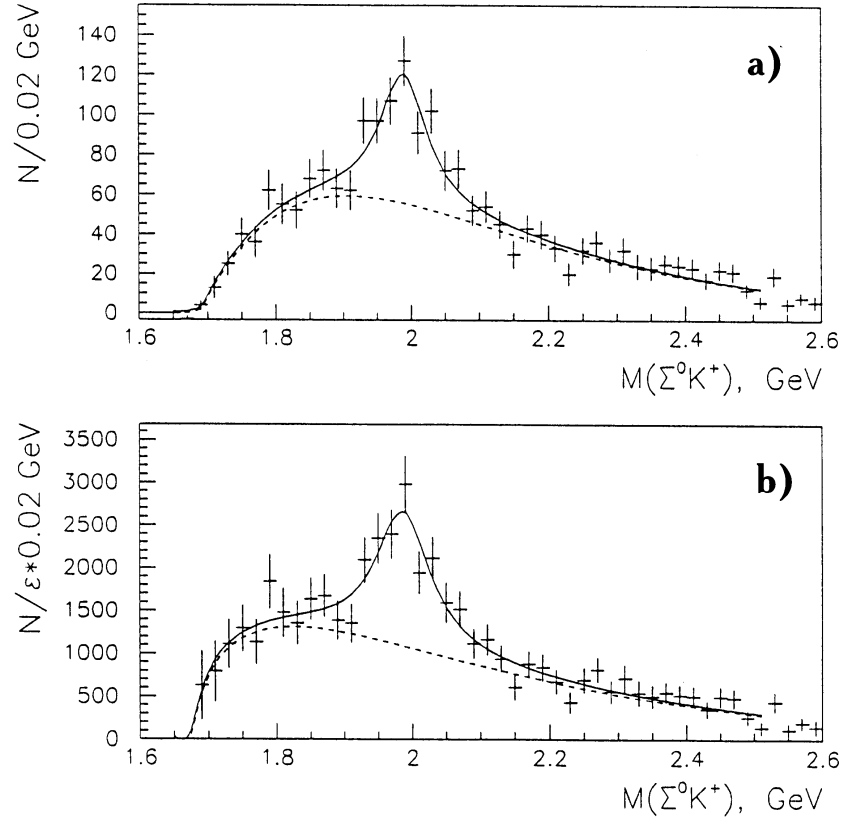


Figure 7: Invariant mass spectra  $M(\Sigma^0 K^+)$  in the diffractive reaction  $p + N \rightarrow [\Sigma^0 K^+] + N$  for all  $P_T^2$  (with soft photon cut): a) measured mass spectrum; b) the same mass spectrum weighted with the efficiency of the setup. Parameters of  $X(2000)$  peak are in Table 2.

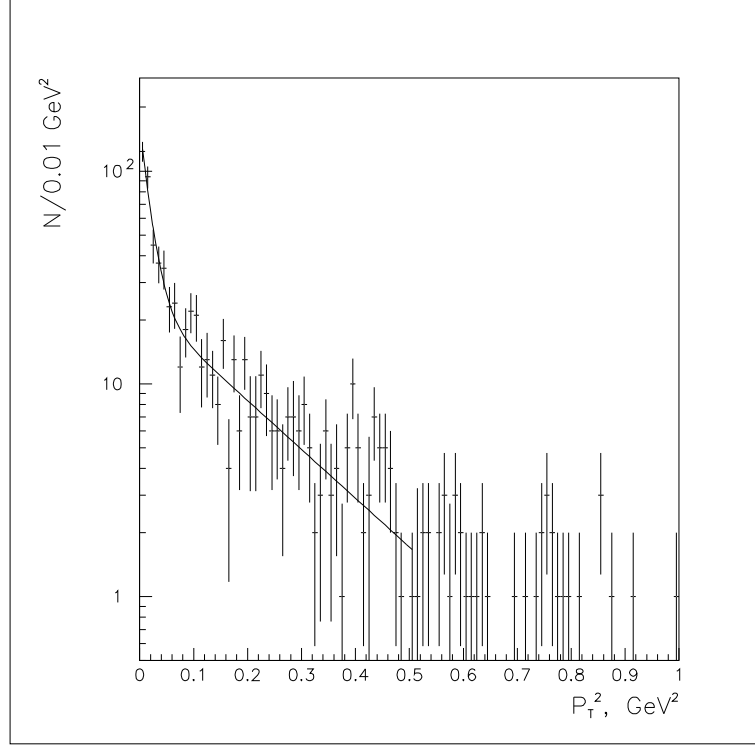


Figure 8:  $dN/dP_T^2$  distribution for the diffractive production reaction  $p + N \rightarrow X(2000) + N$ . The distribution is fitted in the form  $dN/dP_T^2 = a_1 \exp(-b_1 P_T^2) + a_2 \exp(-b_2 P_T^2)$  with the slope parameters  $b_1 = 63 \pm 10 \text{ GeV}^{-2}$ ;  $b_2 = 5.8 \pm 0.6 \text{ GeV}^{-2}$ .

We must bear in mind that it is more convenient to use other relations for cross sections:

$$\sigma[p + N \rightarrow X(2000)^+ + N] \cdot BR[X(2000)^+ \rightarrow (\Sigma K)^+] = 285 \pm 60 \text{ nb/nucleon}, \quad (29)$$

$$\sigma[p + C \rightarrow X(2000)^+ + C] \cdot BR[X(2000)^+ \rightarrow (\Sigma K)^+] = 780 \pm 180 \text{ nb/nucleus}, \quad (30)$$

which were obtained from (27) and (28) using branching ratio (24).

The errors in the cross sections of (27)-(30) are statistical only. Additional systematic errors are  $\simeq \pm 20\%$  due to uncertainties in the cuts, in Monte Carlo efficiency calculations and in the absolute normalization.

In the mass spectra  $M(\Sigma^0 K^+)$  in Fig. 7 there is only a slight indication for  $X(1810)$  structure which was observed earlier in the study of coherent reaction (16) — see Fig. 5 and [21]. This difference is caused by a large background in this region for the events in Fig. 7 (all  $P_T^2$ , soft photon cut). To clarify the situation in this new analysis we investigated also the  $M(\Sigma^0 K^+)$  mass spectra for coherent reaction (16), e.g. for  $P_T^2 < 0.1 \text{ GeV}^2$ . In these mass spectra not only the  $X(2000)$  peak is observed, but the  $X(1810)$  structure as well. These spectra (see [45]) are compatible with the data in Fig. 5.

The yield of the  $X(1810)$  as function of  $P_T^2$  is shown in Fig. 9. From this figure it is clear that  $X(1810)$  is produced only in a very small  $P_T^2$  region ( $P_T^2 < 0.01 - 0.02 \text{ GeV}^2$ ). For  $P_T^2 < 0.01 \text{ GeV}^2$  the  $M(\Sigma^0 K^+)$  mass spectrum demonstrates a very sharp  $X(1810)$  signal (see Fig. 10) with the parameters of the peak

$$X(1810) \rightarrow \Sigma^0 K^+ \begin{cases} M &= 1807 \pm 7 \text{ MeV} \\ \Gamma &= 62 \pm 19 \text{ MeV} \end{cases} \quad (31)$$



which is in a good agreement with the previous data of Table 1. The cross section for coherent X(1810) production is

$$\sigma[p + C \rightarrow X(1810)^+ + C]|_{P_T^2 < 0.01 \text{ GeV}^2} \cdot BR[X(1810)^+ \rightarrow \Sigma^0 K^+] =$$

$$215 \pm 45 \text{ nb/C nucleus.} \quad (32)$$

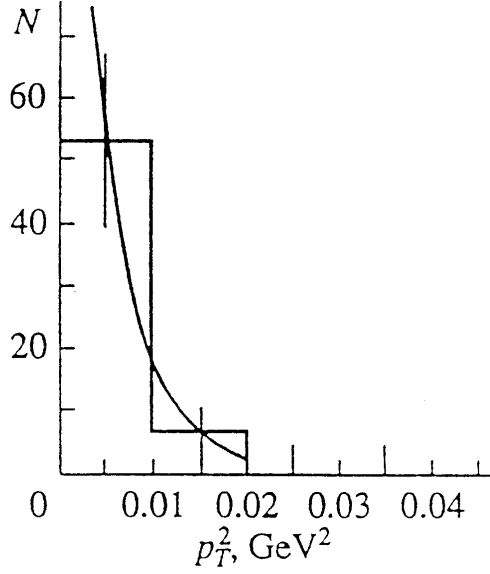


Figure 9: The  $P_T^2$  dependence for the  $X(1810)$  structure production in the coherent reaction  $p + C \rightarrow X(1810) + C$ .

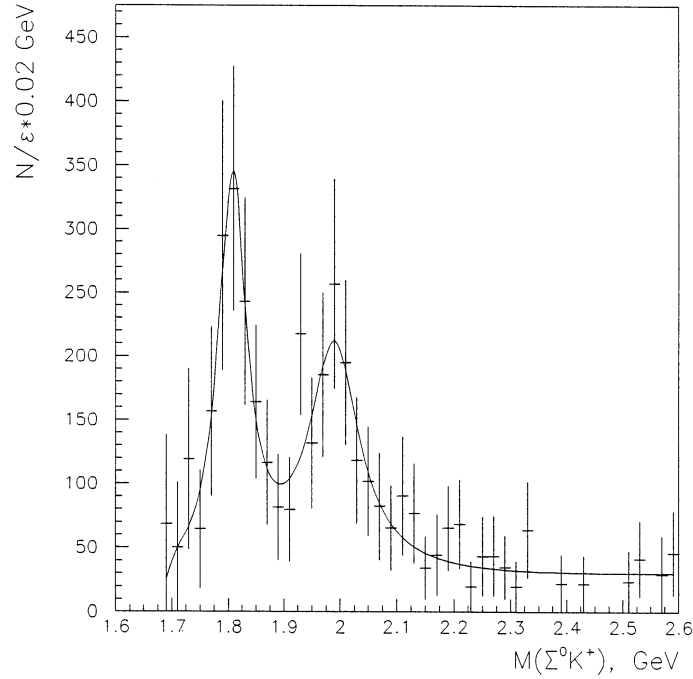


Figure 10: Invariant mass spectra  $M(\Sigma^0 K^+)$  in the coherent diffractive production reaction  $p + C \rightarrow [\Sigma^0 K^+] + C$  in the region of very small  $P_T^2 < 0.01 \text{ GeV}^2$  (with strong photon cut) weighted with the efficiency of the setup.

The additional systematic error for this value is  $\pm 30\%$ . It increased as compared with the same errors in (27)-(30) due to the uncertainty in the evaluation of  $P_T^2$  smearing in the region of  $P_T^2 < 0.01 \text{ GeV}^2$ , which is more sensitive to  $P_T^2$  resolution.

It is possible also to demonstrate the coherent diffractive X(2000) production in the clearest way by using the “restricted coherent region”  $0.02 < P_T^2 < 0.1 \text{ GeV}^2$  (see Fig. 11) where there is no influence of X(1810) structure.

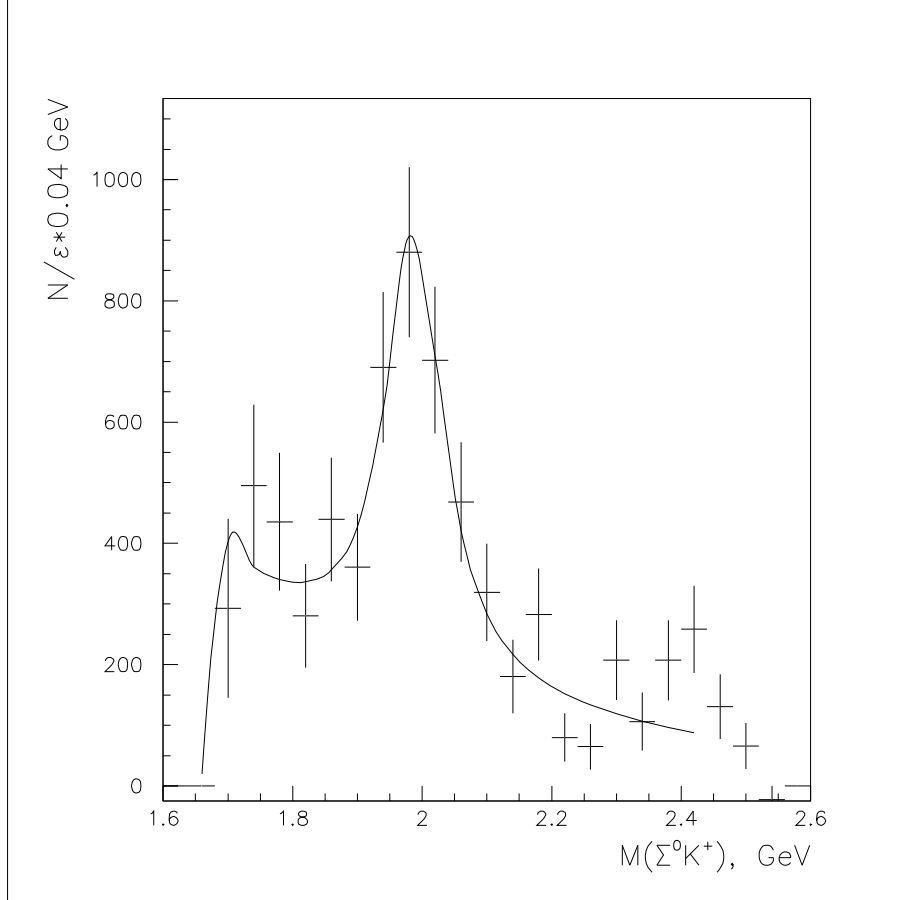


Figure 11: Weighted invariant mass spectrum  $M(\Sigma^0 K^+)$  for the reaction  $p + C \rightarrow [\Sigma^0 K^+] + C$  in the “restricted coherent region”  $0.02 < P_T^2 < 0.1 \text{ GeV}^2$  (with intermediate photon cut).

To explain the unusual properties of X(1810) state in a very small  $P_T^2$  region the hypothesis of the electromagnetic production of this state in the Coulomb field of carbon nucleus was proposed earlier [46]. It is possible to estimate the cross section for the Coulomb X(1810) production from (9) and (10):

$$\begin{aligned} & \sigma[p + C \rightarrow X(1810)^+ + C]|_{P_T^2 < 0.01 \text{ GeV}^2; \text{Coulomb}} = \\ & = (2J_x + 1) \{ \Gamma[X(1810)^+ \rightarrow p + \gamma] [\text{MeV}] \} \cdot 2.8 \cdot 10^{-30} \text{ cm}^2 / \text{C nucleus} \geq \\ & \geq 5.6 \cdot 10^{-30} \text{ cm}^2 \{ \Gamma[X(1810)^+ \rightarrow p + \gamma] [\text{MeV}] \} \end{aligned} \quad (33)$$

( $J_x \geq 1/2$  is the spin of X(1810)).

Let us compare this Coulomb hypothesis prediction with the experimental value

$$\sigma[p + C \rightarrow X(1810)^+ + C]|_{P_T^2 < 0.01 \text{ GeV}^2} \gtrsim 645 \text{ nb/C nucleus}. \quad (34)$$

To obtain (34) we assumed in (16) that  $X(1810)$  is isodoublet, and then we use from (24) the branching  $BR(X^+ \rightarrow \Sigma^0 K^+) \leq 1/3$  (here  $\simeq$  means that  $BR[X^+ \rightarrow (\Sigma K)^+] \simeq 1$ , i.e. this decay is dominating).

If the value of radiative width  $\Gamma[X(1810) \rightarrow p + \gamma]$  is around 0.1-0.3 MeV and the branching  $BR[X(1810)^+ \rightarrow (\Sigma K)^+]$  is significant, then the experimental data for cross section of the coherent  $X(1810)$  production (34) can be in agreement with the Coulomb mechanism prediction (33). It seems that such value of radiative width is quite reasonable. For example, the radiative width for  $\Delta(1232)$  isobar is  $\Gamma[\Delta(1232)^+ \rightarrow p + \gamma] \simeq 0.7$  MeV. The value of radiative width depends on the amplitude of this process  $A$  and on kinematical factor:  $\Gamma = |A|^2 \cdot (P_\gamma)^{2l+1}$  ( $P_\gamma$  is the momentum of photon in the rest frame of the decay baryon and  $l$  is orbital momentum). For  $X(1810) \rightarrow p + \gamma$  decay the kinematical factor may be by an order of magnitude larger than for  $\Delta(1232)^+ \rightarrow p + \gamma$  because of the large mass of  $X(1810)$  baryon. Certainly, the predictions for amplitude  $A$  are quite speculative. But if, for example,  $X(1810)$  is the state with hidden strangeness  $|qqqs\bar{s}\rangle$ , then the amplitude  $A$  might be not very small due to a possible VDM decay mechanism  $(qqqs\bar{s}) \rightarrow (qqq) + \phi_{\text{virt}} \rightarrow (qqq) + \gamma$ . Thus it seems that the experimental data for the coherent production of  $X(1810)$  (34) is not in contradiction with the Coulomb production hypothesis.

It is possible that the candidate state  $X(2050) \rightarrow \Sigma^*(1385)^0 K^+$  which was observed in coherent reaction (14) in the region of very small transverse momenta ( $P_T^2 < 0.02 \text{ GeV}^2$ ) is also produced not by diffractive, but by the electromagnetic Coulomb production mechanism [46].

The feasibility to separate the Coulomb production processes in the coherent proton reactions at  $E_p = 70 \text{ GeV}$  on the carbon target in the measurements with the SPHINX setup was demonstrated recently by observation of the Coulomb production of  $\Delta(1232)^+$  isobar with  $I = 3/2$  in the reaction

$$p + C \rightarrow \Delta(1232)^+ + C \quad (35)$$

(see [46]).

## 6 RELIABILITY OF $X(2000)$ BARYON STATE

(large decay branching with strange particle emission, limited decay width) were obtained with a good statistical significance in different SPHINX runs with widely different experimental conditions and for several kinematical regions of reaction (16). The average values of the mass and width of  $X(2000)$  state are

$$X(2000) \rightarrow \Sigma^0 K^+ \begin{cases} M &= 1989 \pm 6 \text{ MeV} \\ \Gamma &= 91 \pm 20 \text{ MeV} \end{cases} \quad (36)$$

The data on  $X(2000)$  baryon state with unusual dynamical properties

Due to its anomalous properties  $X(2000)$  state can be considered as a serious candidate for pentaquark exotic baryon with hidden strangeness:  $|X(2000)\rangle = |uuds\bar{s}\rangle$ . Recently some new additional data have been obtained which are in favor of the reality of  $X(2000)$  state.

a) In the experiment of the SPHINX Collaboration reaction (17) was studied. The data for the effective mass spectrum  $M(\Sigma^+ K^0)$  in this reaction are presented in Fig. 12. In spite of limited statistics the  $X(2000)$  peak and the indication for  $X(1810)$  structure are seen in this mass spectrum and are quite compatible with the data for reaction (16).

b) In the experiment on the SELEX(E781) spectrometer with the  $\Sigma^-$  hyperon beam of the Fermilab Tevatron the diffractive production reaction

$$\Sigma^- + N \rightarrow [\Sigma^- K^+ K^-] + N \quad (37)$$

was studied at the beam momentum  $P_{\Sigma^-} \simeq 600$  GeV. In the invariant mass spectrum  $M(\Sigma^- K^+)$  for this reaction a peak with parameters  $M = 1962 \pm 12$  MeV and  $\Gamma = 96 \pm 32$  MeV was observed (Fig. 13).

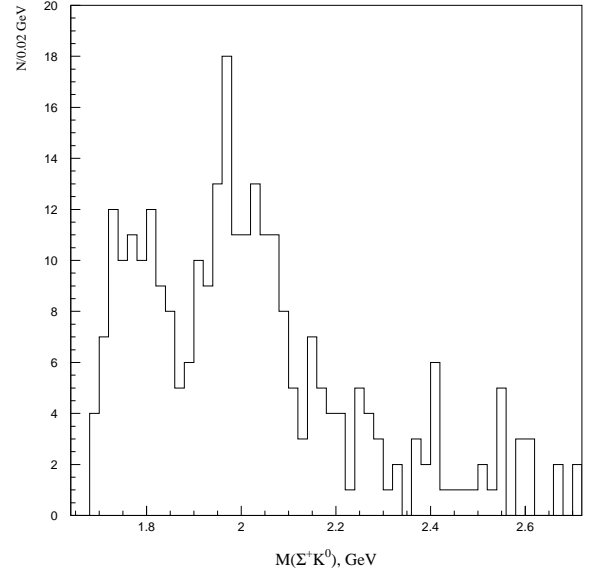


Figure 12: The effective mass spectrum  $M(\Sigma^+ K^0)$  in reaction (17) for  $P_T^2 < 0.1$  GeV<sup>2</sup>.

The parameters of this structure are very near to the parameters of  $X(2000) \rightarrow \Sigma^0 K^+$  state which was observed in the experiments on the SPHINX spectrometer. It seems, that the real existence of  $X(2000)$  baryon is supported by the data of another experiment and in another process.

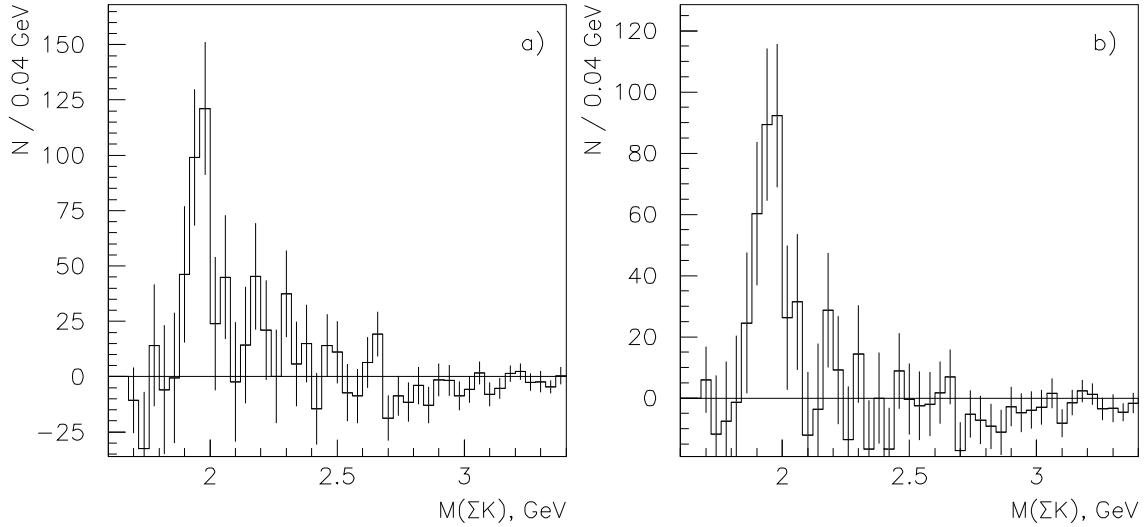


Figure 13: Study of  $M(\Sigma^- K^+)$  in the reaction  $\Sigma^- + N \rightarrow [\Sigma^- K^+ K^-] + N$  in the SELEX experiment. Here the spectrum  $M(\Sigma^- K^-)$  with open exotic quantum number used for subtraction of nonresonance background in  $M(\Sigma^- K^+)$  after some normalization. One presents in this figure  $M(\Sigma^- K^+) - 0.95M(\Sigma^- K^-)$  (here 0.95 — normalization factor): a) all the events; b) after subtraction of the events in  $\phi$  band to suppress the influence of the reaction  $\Sigma^- + N \rightarrow [\Sigma^- \phi] + N$ .

Preliminary results of studying reactions (17) and (37) were discussed in the talks at the last conferences [24,25,47] and are now under detailed study.

## 7 NONPERIPHERAL PROCESSES

As was discussed above (Section 2.3) the search for new baryons in proton-induced diffractive-like reactions in the nonperipheral domain, with  $P_T^2 > 0.3 - 0.5 \text{ GeV}^2$ , seems to be quite promising. Here we present the very first results of these searches in the invariant mass spectra of the  $\Sigma^0 K^+$  and  $p\eta$  systems produced in the reactions  $p + N \rightarrow [\Sigma^0 K^+] + N$  (16) and  $p + N \rightarrow [p\eta] + N$  (18) for  $P_T^2 > 0.3 \text{ GeV}^2$  (see [20,21]). Combined data on reaction (16) from the old and new runs are shown in Fig. 14a. The data from the old run for reaction (18) are shown in Fig. 14b. Despite limited statistics, a structure with mass  $M \approx 2350 \text{ MeV}$  and width  $\Gamma \sim 60 \text{ MeV}$  can be clearly seen in these two mass spectra. They require a further study in future experiments with large statistics. The same statement seems true for intriguing data on the invariant mass spectrum  $M(p\eta')$  for reaction (19) in the region  $P_T^2 > 0.3 \text{ GeV}^2$  (see Fig. 14c). It must be stressed that reaction (19) is the only one (among more than a dozen of other diffractive-like reactions studied in the SPHINX experiments) in which a strong coherent production on carbon nuclei was not observed (the absence of the forward peak in  $dN/dP_T^2$  distribution with the slope value  $b \gtrsim 50 \text{ GeV}^{-2}$ ; the slope for forward cone in (19) is  $b \sim 6.5 \text{ GeV}^{-2}$  — see [20,22]).

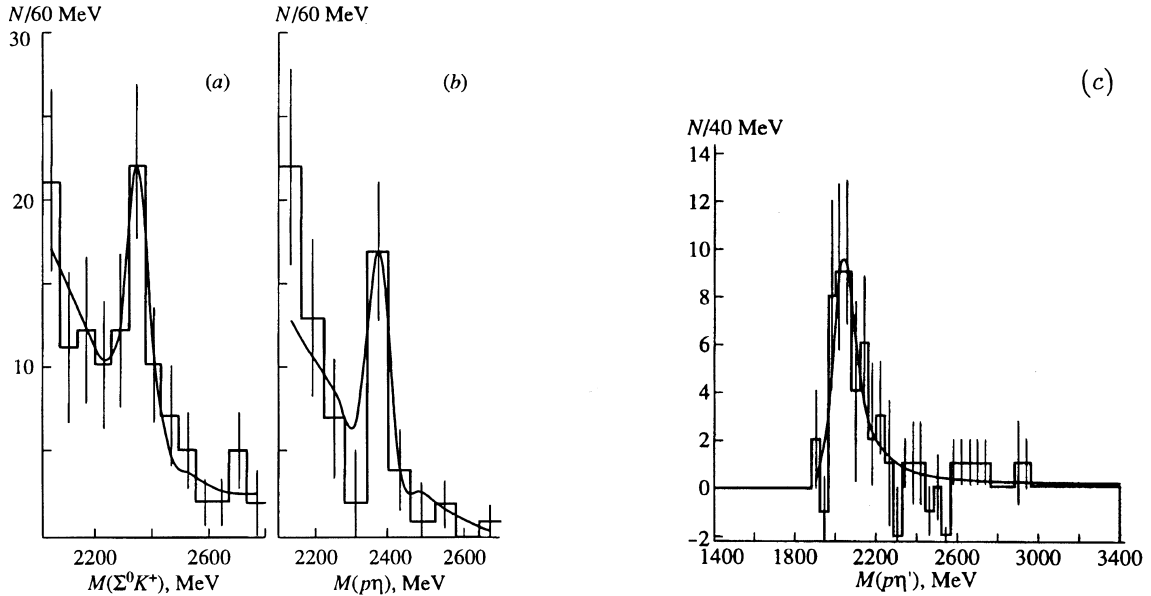


Figure 14: (a) Invariant mass spectrum of the  $\Sigma^0 K^+$  system produced in the reaction  $p + N \rightarrow [\Sigma^0 K^+] + N$  (16) for  $P_T^2 > 0.3 \text{ GeV}^2$  (combined data from the old and new runs). (b) Invariant mass spectrum of the  $p\eta$  system produced in the reaction  $p + N \rightarrow [p\eta] + N$  (18) for  $P_T^2 > 0.3 \text{ GeV}^2$  (old data, see [20]). A narrow structure with  $M \sim 2350 \text{ MeV}$  and  $\Gamma \sim 60 \text{ MeV}$  in the nonperipheral region of reactions (16) and (18) is seen in these mass spectra. (c) Invariant mass spectrum  $M(p\eta')$  for the reaction  $p + N \rightarrow [p\eta'] + N$  (19) in the region  $P_T^2 > 0.3 \text{ GeV}^2$  (old run). This spectrum is dominated by a threshold structure with  $M \sim 2000 \text{ MeV}$  and  $\Gamma \sim 100 \text{ MeV}$ .

## CONCLUSION

The extensive research program of studying diffractive production in  $E_p = 70 \text{ GeV}$  proton reactions is being carried out in experiments with the SPHINX setup [2, 12-28, 45-47]. This program is aimed

primarily at searches for cryptoexotic baryons with hidden strangeness ( $|uuds\bar{s}\rangle$ ). Only a part of these experiments is discussed here.

The most important results of these searches were obtained in studies of the hyperon-kaon systems produced in proton diffractive dissociation processes and first of all in reaction  $p + N \rightarrow \Sigma^0 K^+ + N$  (16).

New data for this diffractive production reaction were obtained with the partially upgraded SPHINX detector (with new  $\gamma$ -spectrometer and with better possibilities to detect  $\Lambda \rightarrow p\pi^-$  and  $\Sigma^0 \rightarrow \Lambda\gamma$  decays). New data are in a good agreement with previous SPHINX results on the invariant mass spectrum  $M(\Sigma^0 K^+)$  in this reaction.

A strong  $X(2000)$  peak with  $M = 1989 \pm 6$  MeV and  $\Gamma = 91 \pm 20$  MeV together with a narrow threshold structure (with  $M \sim 1810$  MeV and  $\Gamma \sim 60$  MeV) are clearly seen in the  $(\Sigma^0 K^+)$  invariant mass spectra. The latter structure is produced at very small transverse momenta,  $P_T^2 < 0.01 - 0.02$  GeV<sup>2</sup>. Unusual properties of the  $X(2000)$  baryon state (narrow decay width, anomalously large branching ratio for the decays with strange particle emission) make this state a serious candidate for a cryptoexotic pentaquark baryon with hidden strangeness  $|qqqs\bar{s}\rangle$ . Preliminary data for  $|\Sigma K\rangle$  states in other reactions (17) and (37) confirm the real existence of  $X(2000)$  baryon.

Several other interested phenomena were observed in the nonperipheral domain (with  $P_T^2 \gtrsim 0.3$  GeV<sup>2</sup>), in the study of different reactions (for example, reactions (14), (18) and (19)). But they need experimental verification with much better statistics.

Now the first stage of the experimental program on the SPHINX setup has been completed. In the last years the SPHINX spectrometer was totally upgraded. The luminosity and the data taking rate were greatly increased. In the recent runs with this upgraded setup we obtained a large statistics which is now under data analysis. In the near future, we expect to increase statistics by an order of magnitude for the processes discussed above and for some other proton reactions.

This work is partially supported by Russian Foundation for Basic Research.

## References

- [1] L.G.Landsberg. Surv. High Energy Phys. 6(1992), 257.
- [2] L.G.Landsberg. Yad.Fiz. 57 (1994) 47 [Phys. At. Nucl. (Engl.Transl.) 57 (1994) 42]; USP. Fiz. Nauk. 164 (1994) 1129. [Physics-Uspekhi (Engl. Transl.) 37 (1994) 1043].
- [3] K.Peters. Nucl. Phys. A558 (1993) 92.
- [4] C.B.Dover. Nucl. Phys. A558 (1993) 721.
- [5] C.Amsler. Rapporter talk. Proc. Conf on High Enerhy Phys. (ICHER), Glasgow, Scotland, July 1994.
- [6] F.E.Close. Preprint RAL-87-072, Chilton, 1987.
- [7] P.Blum. Int. J.Mod. Phys. 11 (1996), 3003.
- [8] T.Hirose et. al. Nuov. Cim. 50 (1979) 120; C.Fucunage et al. Nuov. Cim. 58 (1980) 199.
- [9] J.Amizzadeh et al. Phys. Lett. B89 (1979) 120.
- [10] A.N.Aleev. et al. Z.Phys. C25 (1984) 205.
- [11] V.M.Karnaukhov V.M. et al. Phys. Lett. B281 (1992) 148.

- [12] D.V.Vavilov et al. (SPHINX Collab.). *Yad. Fiz.* 57 (1994) 241 [*Phys. At. Nucl. (Engl. Transl.)* 57 (1994) 227]; M.Ya.Balatz et al. (SPHINX Collab.). *Z.Phys.* C61 (1994) 220.
- [13] M.Ya.Balatz et al. (SPHINX Collab.). *Z.Phys.* C61 (1994) 399.
- [14] D.V.Vavilov et al. (SPHINX Collab.). *Yad. Fiz.* 57 (1994) 253 [*Phys. At. Nucl. (Engl. Transl.)* 57 (1994) 238].
- [15] L.G.Landsberg et al (SPHINX Collab.). *Nuov. Cim.* A107 (1994) 2441.
- [16] V.F.Kurshetsov, L.G.Landsberg. *Yad. Fiz.* 57 (1994) 2030 [*Phys. At. Nucl. (Engl. Transl.)* 57 (1994) 1954].
- [17] D.V.Vavilov et al. (SPHINX Collab.). *Yad. Fiz.* 57 (1994) 1449 [*Phys. At. Nucl. (Engl. Transl.)* 57 (1994) 1376].
- [18] D.V.Vavilov et al. (SPHINX Collab.). *Yad. Fizz.* 58 (1995) 1426 [*Phys. At. Nucl. (Engl. Transl.)*] 58 (1995) 1342.
- [19] S.V.Golovkin et al. (SPHINX Collab.). *Z. Phys.* C68 (1995) 585.
- [20] S.V.Golovkin et al. (SPHINX Collab.). *Yad. Fiz.* 59 (1996) 1395 [*Phys. At. Nucl. (Engl. Transl.)*. 59 (1996) 1336].
- [21] V.A.Bezzubov et al. (SPHINX Collab.). *Yad. Fiz.* 59 (1996) 2199 [*Phys. At. Nucl. (Engl. Transl.)*. 59 (1996) 2117].
- [22] L.G.Landsberg. *Yad. Fiz.* 60 (1997) 1541. [*Phys. At. Nucl. (Engl. Transl.)*. 60 (1997) 1397].
- [23] L.G.Landsberg. *Hadron Spectroscopy ("Hadron 97")*. Seventh Intern. Conf. Upton, NY, August 1997 (ed. S.-U.Chung, H.J.Willutzki), p. 725.
- [24] L.G.Landsberg. *Proc. of 4th Workshop on Small-X and Diffractive Physics, Fermilab, Batavia, 17-20 September 1998*, p.189.
- [25] L.G.Landsberg. Plenary Talk on the Conf. "Fundamental Interactions of Elementary Particles", ITEP, Moscow, November 1998. *Yad. Fiz.* (in press).
- [26] V.A.Victorov et al. *Yad. Fiz.* 59 (1996) 1229 [*Phys. At. Nucl. (Engl. Transl.)* 59 (1996) 1175].
- [27] M.Ya.Balatz et al. (SPHINX Collab.). *Yad. Fiz.* 59 (1996) 1242 [*Phys. At. Nucl. (Engl. Transl.)* 59 (1996) 1186].
- [28] S.V.Golovkin et al. *Z. Phys.* A359 (1997) 435.
- [29] Hong-Mo Chan and H.Hogaasen. *Phys. Lett.* B72 (1977) 121; Hong-Mo Chan et al. *Phys. Lett.* B76 (1978) 634.
- [30] H.Hogaasen and P.Sorba. *Nucl. Phys.* B145 (1978) 119; Invited Talk at Conf. on Hadron Interactions at High Energy. Marseilles (France) 1978.
- [31] M.De Crombrughe et al. *Nucl. Phys.* B156 (1979) 347.
- [32] Hong-Mo Chan, S.T.Tsou. *Nucl. Phys.* B118 (1977) 413.

- [33] C.Caso et al. (PDG). The Europ. Phys. Journ., 3 (1998) 1.
- [34] L.G.Landsberg. Usp. Fiz. Nauk. 160 (1990) 1.
- [35] G.Bellini et al. Nuov. Cim. A79 (1984) 282.
- [36] D.Alde et al. (GAMS Collab.) Phys. Lett. B182 (1986) 105; Phys. Lett. B276 (1992) 457.
- [37] D.Alde et al. (GAMS Collab). Phys. Lett. B216 (1989) 447; Phys. Lett. B276 (1992) 375.
- [38] S.S.Gershtein. Proc. 3rd Int. Conf. on Hadron Spectroscopy: "Hadron-89" (Eds. F. Binon et al.) Paris (1989) 175.
- [39] R.A.Shumacher. Preprint CMU MEG-96-007, Pittsburg, 1996.
- [40] H.Primakoff. Phys. Rev. 81 (1951) 899.
- [41] I.Ya.Pomeranchuk and I.M.Shmushkevitch. Nucl. Phys. B23 (1961) 452.
- [42] A.Halpern et al. Phys. Rev. 152 (1966) 1295; J.Dreitlein, H.Primakoff. Phys. Rev. 125 (1962) 591.
- [43] M.Zielinski et al. Z.Phys. C31 (1986) 545; C34 (1986) 255.
- [44] L.G.Landsberg. Nucl. Phys. (Proc. Suppl.) B211 (1991) 179c; Yad. Fiz. 52 (1990) 192.
- [45] S.I.Golovkin et al. Europ. Phys. Journ. A (to be published).
- [46] D.V.Vavilov et al. Yad. Fiz. 62 (1999) (to be published).
- [47] G.S.Lomkazi. Talk on the Symposium on Modern Trends in Particles Physics, dedicated to the 70 anniversary of G.Chikovani. Tbilisi, Georgia, September 1998.